Long open path measurements of greenhouse gases in air using near infrared Fourier transform spectroscopy

David W. T. Griffith[1], Denis Pöhler[2], Stefan Schmitt[2], Samuel Hammer[2], Sanam N. Vardag[2,3], and Ulrich Platt[2]

5 [1] Centre for Atmospheric Chemistry, University of Wollongong, Australia
[2] Institute of Environmental Physics, University of Heidelberg, Germany
[3] now at Heidelberg Center for the Environment, University of Heidelberg, Germany

Correspondence to: David Griffith (Griffith@uow.edu.au)

10 **Abstract**

In complex and urban environments, atmospheric trace gas composition is highly variable in time and space. Point measurement techniques for trace gases with in situ instruments are well established and accurate, but do not provide spatial averaging to compare against developing high resolution atmospheric models of composition and small scale meteorology with resolutions of the order of a kilometre. Open path measurement techniques provide path average concentrations and

15 spatial averaging which, if sufficiently accurate, may be better suited to assessment and interpretation with such models. Open path Fourier Transform Spectroscopy (FTS) in the mid infrared region, and Differential Optical Absorption Spectroscopy (DOAS) in the UV and visible, have been used for many years for open path spectroscopic measurements of selected species in both clean air and in polluted environments. Compared to the mid infrared, near infrared instrumentation allows measurements over longer paths than mid IR FTS, for species such as greenhouse gases which are not easily

20 accessible to DOAS.

In this pilot study we present the first open path near infrared (4000-10,000 cm^{-1}, 1.0 – 2.5 μm) FTS measurements of CO_2, CH_4, O_2, H_2O and HDO over a 1.5 km path in urban Heidelberg, Germany. We describe the construction of the open path FTS system, the analysis of the collected spectra, precision and accuracy of the measurements, and the results from a four-month trial measurement period in July-November 2014. The open path measurements are compared to calibrated in situ

25 measurements made at one end of the open path. There are small but significant differences between in situ and open path measurements coincident in time which reflect local sources and sinks and the way in which they are sampled by the point and path-averaged measurements. Open path FTS may provide a valuable new tool for investigations of atmospheric trace gas composition in complex, small scale environments such as cities.

Introduction

The cycling of carbon between Earth's surface and the atmosphere is dominated by carbon dioxide (CO_2) and methane (CH_4), which are also the two most important anthropogenically-influenced greenhouse gases. The steady increases in atmospheric CO_2 and CH_4 concentrations in the global atmosphere since industrialisation have been well documented by the global network of surface in situ point measurements (e.g.GLOBAL-VIEW-CO_2, 2009). Such point-based in situ measurements in clean baseline air are well suited to monitoring long term global changes in atmospheric greenhouse gases (including also nitrous oxide (N_2O) and other minor species), and have provided most of the data from which long term global trends have been assessed. However to characterise and quantify individual sources and sinks of greenhouse gases, measurements in regional, urban, agricultural and industrial environments located near the sources and sinks, combined with fine-resolution local and regional-scale atmospheric transport modelling, are required. In recent work, Turner et al. (2016) concluded from a modelling study that a dense (2 km) fixed network of point sensors with only moderate precision was sufficient to characterise CO_2 sources with 5% accuracy in the San Francisco Bay area. Lee et al. (2016) trialled a network of five mobile CO_2 sensors in the Vancouver urban area combined with an aerodynamic model to calculate fluxes.

Point measurements are sensitive to the immediate local environment, and may or may not adequately represent the mean concentrations over the grid-scale of the relevant atmospheric models in non-background environments. Open path (OP) measurements provide spatially averaged concentrations by measuring an optical absorption spectrum along a path between a light source and the measuring instrument and retrieving component concentrations from the spectra. Spatial averaging at similar scales to those of the finest urban and regional scale models should be advantageous in combining measurements and models to deduce the strengths of localised sources and sinks of greenhouse gases. But how accurately can we measure such spatially averaged trace gas concentrations?

The longest-established surface OP techniques (i.e. excluding satellite and ground based total column measurements) are Differential Optical Absorption Spectroscopy (DOAS), typically employing the UV and visible spectral regions (Platt and Stutz, 2008), and Open Path -Fourier Transform Spectroscopy (OP-FTS) in the mid infrared (e.g. Tuazon et al., 1978; Russwurm and Childers, 2002; Griffith and Jamie, 2006). While DOAS can operate over pathlengths of several kilometres, suitable absorptions for accurate and precise measurements of CO_2, CH_4 and other GHGs are not available in the UV-visible spectrum. In the mid IR suitable absorptions are available, but when restricted to conventional broadband blackbody sources such as a globar, low source brightness limits beam collimation across the open path and restricts pathlengths to typically a few hundred metres. Until recently the near infrared (NIR) region has been little used. The NIR allows the use of a high temperature, bright white light source (such as quartz halogen or Xe lamp) allowing good beam collimation over kilometre-scale pathlengths, but absorption strengths of the available overtone and combination vibrational spectral bands are much lower than for the fundamental transitions in the mid IR. Previous work to extend DOAS into the NIR region using a conventional white-light source, monochromator and detector array was limited by the weak absorptions and interfering spectral structures to an accuracy of approximately 30% for CO_2 and CH_4 (Sommer, 2012). More recently, DOAS- type NIR

measurements using broadband laser sources (Saito et al., 2015; Somekawa et al., 2011), and frequency comb spectroscopy (Rieker et al., 2014; Waxman et al., 2017) have been described to measure CO_2 and CH_4 in the NIR over pathlengths of up to 5 km. These methods achieved measurement precisions of 1-4 ppm with absolute differences of up to 7 ppm for CO_2 when compared to point in situ measurements.

5   The recent and rapid development of TCCON, the Total Carbon Column Observing Network (Wunch et al., 2011) has shown that the near IR spectrum with a ground based FT spectrometer and the sun as a source is suitable for highly accurate and precise (<0.5%) measurements of total column CO_2, CH_4, N_2O and other trace gases. Smith et al., (2011) assessed the performance of OP-FTS in the mid infrared, finding accuracies of a few percent without calibration against standards. In this work, drawing on our combined experience in TCCON, mid IR OP-FTS and DOAS, we describe measurements of CO_2,

10   CH_4, H_2O, HDO, O_2 and other gases with a Fourier Transform Spectrometer (FTS) operating in the near infrared (4000-10000 cm^{-1}, 1.1 – 2.5 μm) using a simple broad-band halogen light source combined with a long open path telescope and retro reflector system over a 1.5 km path (one-way, 3.1 km total absorption pathlength) in urban Heidelberg, Germany. The spectroscopy is similar to that used in TCCON, and in this pilot study we aimed to (1) assess the precision, accuracy and stability of such ground based long open path measurements and (2) compare and test for biases between open path

15   measurements and point measurements made with a calibrated in situ analyser at one end of the open path. The measurement system operated for 4 months from July – November 2014 in urban Heidelberg, Germany.

2 Experimental

2.1 FT Spectrometer and long path optics

The optical system is shown schematically in Figure 1. The spectrometer and telescope were located in the rooftop

20   observatory on the 6-storey Institute of Environmental Physics (IUP) on the University of Heidelberg campus in urban Heidelberg, (49.4172°N, 8.6745°E, 145 masl, 33 m above ground) and the retroreflector array on the Institute of Physics (PI) building 1555 m east at (49.4149°N, 8.6956°E, 169 masl). The distance was measured with a laser rangefinder to 1 m accuracy. The intervening path is illustrated in Figure 2 and crossed above a residential area approximately 0.5 km north of the Neckar River and 1.5 km NE of the Heidelberg city centre. A 35W tungsten-quartz-halogen source was focussed by a 25

25   mm focal length, 25 mm diameter NIR-coated glass lens (Edmund Scientific, not shown) into a 6 x 200 μm fibre bundle (3 m long, 200/240 IRAN, Loptec GmbH) and directed to the primary focus of a 300 mm diameter, 150 cm focal length Newtonian telescope (aluminium primary mirror with SiO_2 overcoat). The collimated beam from the telescope was directed via fine step-control alignment motors to an array of 17 x 63 mm diameter UV solid quartz cornercubes which acted as retroreflectors to return the beam to the telescope. The focussed return beam was collected by a single 200 μm fibre in the

30   centre of the 6-fibre bundle in the same sheath, which forked to direct the single fibre to the input of the FT spectrometer.

The fibre coupling to the telescope is described in detail by Merten et al. (2011). In practice the fibre end at the telescope was slightly defocussed to maximise the light throughput to the spectrometer.

The return beam from the fibre was focussed by a 75 mm focal length NIR-coated lens into the 1 mm entrance stop of the FT spectrometer (IRcube, Bruker Optics, Ettlingen Germany) which had a quartz beamsplitter and InGaAs detector optimised for the NIR spectral region (3800 – 10000 cm^{-1}). An overview of a typical spectrum is shown in Figure 3. The lower frequency cutoff was determined by the transmission of the quartz cornercubes and fibres.

Measurements reported here were collected continuously from 10 July – 4 November 2014. Spectra were recorded with a resolution of 0.55 cm^{-1} (maximum optical path difference 1.8 cm), each coadding 84 scans over 5 minutes. Each hour a background stray light spectrum was recorded by blocking the source at the fibre input and a short path reference spectrum was recorded by blocking the beam at the telescope end of the fibre with an aluminium diffuse reflector plate to return a small fraction of the intensity to the detector without traversing the long open path. Over the 4 month measurement period over 26,000 spectra were collected, of which approx. 3000 were rejected due to poor visibility and low signal or other, normally weather-related effects. In total we collected and analysed usable data for 60% of the available time.

Atmospheric pressure and temperature for the measurement path, required for the spectrum analysis and to calculate air density, were measured and averaged over the period of each spectrum measurement by an electronic barometer (Vaisala PTB110) and LM335 diode respectively, co-located with the FT spectrometer. The acquisition of spectral data, pressure and temperature, shutter control and real-time spectrum analysis were executed automatically by the software available for the Ecotech Spectronus in situ FTIR analyser (Ecotech, Knoxfield , Australia). Initially the IUP weather station temperature and height-adjusted pressure were used in the spectrum analysis; the weather station temperature was subsequently replaced by the path-averaged temperature derived from the spectra themselves, as described below.

2.2 In situ trace gas measurements

At the IUP end of the open path, air from a roof-level inlet on the IUP building was sampled and analysed continuously with an in situ trace gas analyser described in detail elsewhere (Griffith et al., 2012; Hammer et al., 2013; Vardag et al., 2015). This analyser is based on an FTIR spectrometer operating in the mid-IR and provided simultaneous high precision measurements of CO_2, CH_4, CO, N_2O, $\delta^{13}C$ and $\delta^{18}O$ in CO_2 calibrated against WMO-GAW standards and provided calibrated point measurements for comparison with the path averaged open path measurements. Measurements were made continuously, averaged every 3 minutes, and the time series was interpolated to the mean times of the open path measurements for point-by-point comparison.

Meteorological measurements

Standard measurements of pressure, temperature, humidity, wind speed, wind direction and solar radiation were obtained from the IUP weather station located on the roof of the building as 5 minute averages and interpolated to the times of the open path measurements.

2.3 Spectrum analysis and retrieval of trace gas amounts

Path averaged trace gas mole fractions were retrieved from spectra by iteratively best-fitting a calculated spectrum to the measured spectrum. The forward model, MALT (Griffith, 1996) calculates the transmission spectrum from a set of input parameters including absorption line parameters, trace gas amounts, pressure, temperature and pathlength as well as

5   instrument parameters including resolution, apodisation function, lineshape, spectral shift and a polynomial fit to the continuum, which in these single beam spectra is generally not flat. The line parameters are based on Hitran 2008 (Rothman et al., 2009) updated by Toon and co-workers for the GFIT software used throughout TCCON (Wunch et al., 2015). The inverse model uses non-linear least squares following the Levenberg-Marquart algorithm (Press et al., 1992) to retrieve the path averaged concentration of each trace gas species. The path averaged concentrations are converted to mole fractions by

10   dividing by the concentration of air determined from pressure and temperature. More details are given by Griffith et al. (2012).

Details of the spectral windows used for the NIR long path analysis are summarised in Table 1 and typical fits for spectral regions used to retrieve O_2, CO_2 and CH_4 are shown in Figure 4. Note these spectral windows are quite different from those used in the mid-IR in the in situ analyser (Griffith et al., 2012).

15   Background spectra of stray light measured hourly by blocking the source had intensities up to 1% of those of the open path spectra, maximising in the early morning and late evening when the solar elevation was low and direction roughly parallel (E-W) to the open path. Scattered solar stray light collected by the FTIR spectrometer has an effective atmospheric path of 8 – 30 km depending on zenith angle, leading to stronger path-average trace gas absorption and higher apparent column amounts of trace gases retrieved from the spectra – for CO_2 the enhancement can be up to 5 ppm at low sun elevations with

20   an additional spike apparent when the near-direct solar beam is captured (see example for O_2 below). The enhancement is typically less than 1-2 ppm during the middle of the day and at night. The analyses were not corrected for stray light because (a) the stray light spectra were measured only once per hour so we do not get an accurate measurement of the scattered light at the time of each 5 minute OP measurement, and (b) the stray light spectrum is weak and noisy and adds noise to the retrieved trace gas amounts from the measurements. An improvement to the optical configuration to avoid scattered light

25   interference is described below under future directions.

2.4 Path averaged temperature measurement

Significant differences of up to 5°C became apparent between measurements of temperature from the point sensors located at the instrument and at the weather stations at each end of the optical path. An effective path-averaged temperature for each measurement is preferable to a point measurement, and was therefore retrieved from the spectra themselves by allowing

30   temperature to be an adjustable parameter in the least-squares fit. The IUP station temperature was used as the initial estimate for the fit. Temperature was retrieved from the CO_2 window at 4980 cm^{-1} (Figure 4b) which has good signal to noise ratio and absorption lines with a range of temperature sensitivities. Figure 5 illustrates typical temperatures and

differences over a period of four sunny days – there is a systematic offset, with the point measurement always higher relative to the path average, and larger differences during daytime. This may be due to the thermal mass of the building on which the weather station was located or radiative heating of the sensor, while the open optical path is typically 10-30 m above the ground and buildings in free air. We expect the retrieved path averaged temperature to be a better estimate of the true path averaged temperature; this is confirmed when used to fit O_2 as described further below, as it led to less apparent diurnal variability in the retrieved O_2. The CO_2-spectrum-derived path-average temperatures were therefore used in all spectrum re-analyses in other spectral regions.

2.5 Instrument lineshape (ILS) characterisation

To check the instrument lineshape function (ILS) of the FTS, we followed Frey et al. (2015), by measuring the spectrum of water vapour in a short-path reference spectrum over a pathlength in air of approximately 3 m and fitting it using both MALT and Linefit (Hase et al., 1999) programs. Assuming the nominal field of view (FOV) of the FTS of 7.2 mrad, we found a linear drop in modulation efficiency to 0.67 at the maximum optical path difference. Alternatively, setting the modulation to its nominal value of 1.0 and fitting the field of view, we retrieved an effective FOV of 10.8 mrad. The effective ILS width is thus approximately 30% broader than the nominal value for a perfect optical system. This is consistent with the short focal length optics and aberrations in the compact optical system. The ILS is shown in Figure 6. The full width at half height is 0.58 cm^{-1}, equivalent to 0.12 nm at 7000 cm^{-1} (1428 nm) and 0.24 nm at 5000 cm^{-1} (2000 nm).

3 Results

3.1 Oxygen, O_2

Retrieval of the O_2 mole fraction from the 1.27 μm (7880 cm^{-1}) band (Figure 4a) provides a system check since the O_2 mole fraction is constant and well known, 0.2095 relative to dry air. Initial retrievals using the weather station pressure and temperature displayed diel variations of the order of 1-2% that were reduced significantly using path-averaged temperatures derived from the CO_2 spectrum fit, as described above. The O_2 measurements for the whole period are shown in Figure 7. The positive spikes observed regularly near 18:00-19:00 local time on clear sunny days are due to direct sunlight scattered into the detector as described in the previous section - when the solar beam path is from the west at low elevation and approximately aligned with the optical path (Figure 2), solar radiation is back-reflected from the retroreflectors and captured by the telescope. Corresponding spikes are also seen in CO_2 and CH_4 records.

The mean mole fraction (excluding evening scattered sunlight anomalies) is 0.217, a bias of +3.6% from the known value of 0.2095. This is larger than the +2% bias found consistently at all TCCON sites, where it is attributed to inaccuracies in the spectroscopic line parameters (Wunch et al., 2010).

3.2 Water vapour, H_2O and HDO

Water vapour provides a further check of the FTS measurements against weather station humidity. (The in situ analyser does not measure ambient water vapour as the sample is dried for measurement.) H_2O and its deuterated isotopologue HDO were co-fitted in a window 4910 - 5080 cm^{-1} (Figure 4b, Table 1) and results are shown in Figure 8. δD was calculated as

$$\delta D = \left(\frac{(HDO/H_2O)_{air}}{(HDO/H_2O)_{SMOW}} - 1 \right) * 1000‰$$

where $(HDO/H_2O)_{air}$ is the measured isotopologue ratio and $(HDO/H_2O)_{SMOW}$ is the corresponding reference ratio for Standard Mean Ocean Water. The spectroscopically measured water vapour amount is in excellent agreement with the weather station record, with a 6% high bias which may be due in part to the humidity sensor accuracy. The uncalibrated mean δD is -68 ± 59 ‰, somewhat higher than recent summer measurements near Zurich, 230 km south of Heidelberg, -120 to -180 ‰ (Aemisegger et al., 2012). However the precision of the δD measurements is not sufficient to distinguish any variability related to temperature, and we do not analyse the δD results further here.

3.3 Carbon dioxide, CO_2

The OP dry air mole fractions retrieved from the spectra are shown in Figure 9 together with the calibrated in situ measurements at the IUP (western) end of the open path. The raw OP measurements are systematically higher than the in situ measurements, which are calibrated against WMO reference standards. We assume this to be a measurement bias due to the difference between the SI-traceable WMO scale of the in situ measurements and the uncalibrated OP measurements which are derived from spectrum fitting based on Hitran line parameter data. To estimate the bias, we take the mean ratio of the OP to calibrated in situ measurements at wind speeds above 6 m s^{-1} when the atmosphere is most likely to be well mixed and real differences between point and open path measurements are minimal. The bias is 2.5% (~ +10 ppm) and all raw OP data are scaled down by a factor of 1.025 in Figure 9 and the following discussion.

The short term peak-to-peak variability in OP CO_2 measurements during periods of little systematic variability is ~5 ppm, corresponding to a 1σ uncertainty of approximately 1.5 ppm (5 min averaging time) assuming the variability is normally distributed. We take this value as an estimate of the instrumental measurement noise - it is an upper limit as it may include real atmospheric variability. The 1σ repeatability of the in situ measurements is ten times smaller, of the order of 0.1 ppm CO_2 (Griffith et al., 2012).

Figure 10 shows differences between the bias-corrected open path and in situ measurements of CO_2 (a) vs wind speed, (b) vs wind direction, and (c) as a histogram. From Figure 10(a) differences are generally smaller at higher windspeeds when the atmosphere is best mixed. The standard deviation of the differences at windspeeds >6 m s^{-1} is around 5 ppm, ~3 times greater than the measurement noise. We suggest differences greater than ~5 ppm to be significant real differences between the OP and in situ measurements, but cannot exclude that some of the differences may be due to instrumental effects. At low

windspeeds (< 2 m s^{-1}), the differences can be over 40 ppm but 98% of absolute differences are less than 20 ppm. The differences appear approximately normally distributed with a small negative bias of ~ -2 ppm, discussed in section 4.2.

3.4 Methane, CH$_4$

Similar analyses for CH$_4$ as for CO$_2$ are shown in Figure 11 and Figure 12. In this case there is a significant positive tail in the distribution of differences at all windspeeds which increases the mean OP - in situ difference for windspeeds >6 m s^{-1}. We have therefore bias-corrected the OP CH$_4$ data with the mean for windspeeds > 2 m s^{-1} where the influence of the tail in the mean is less. The mean scale factor is 1.007 (~ 13 ppb) and the 1σ measurement precision estimated from the short term peak-to-peak noise is ~ 40 ppb. The standard deviation of the OP – in situ differences is 93 ppb; as for CO$_2$ this is around twice the underlying measurement noise and can be attributed to real atmospheric differences.

3.5 Carbon monoxide, CO

Absorption by the quartz retroreflectors below 4600 cm^{-1} in the region of the CO overtone band centred near 4300 cm^{-1} prevents analysis of CO from these spectra. With more appropriate IR quartz, glass or hollow mirror retroreflectors of higher transmission in this region, a simulation of the resultant expected spectra based on the performance achieved with the current system suggests CO measurements with a 5-minute measurement averaging time would provide repeatability of the order of 5-10 ppb, which would be sufficient precision in polluted urban environments.

3.6 Nitrous oxide, N$_2$O

N$_2$O absorbs only weakly in the NIR. Analysis of the spectra in the strongest available band centred at 4730 cm^{-1} provides a mean and standard deviation of the N$_2$O mole fraction over the whole measurement period of 353 ± 680 ppb. While the mean is realistic, the precision is not sufficient to detect meaningful changes in N$_2$O amounts, which are small (a few ppb) due to the weak sources and sinks and long lifetime of N$_2$O. A stronger band near 4415 cm^{-1} would become accessible with glass retroreflectors, but would provide only a factor of two improvement.

4 Discussion and Conclusions

4.1 Precision, accuracy and open-path – in situ differences

Table 2 summarises several measures of precision and accuracy of the OP-FTS system for CO$_2$, CH$_4$ and O$_2$ measurements over the 1.55 km one-way, 3.1 km return path. Precision of the OP measurements (random error, 1σ repeatability) is estimated as one quarter of the observed peak-peak variability for each species during periods of little apparent systematic variability – 0.4% for CO$_2$, 2.2% for CH$_4$ and 2.5% for O$_2$. During these periods in situ measurement variability is smaller by a factor of three or more. These are upper limits as they may include real atmospheric variability. When OP measurements

are compared to in situ measurements at the IUP (western) end of the path, CO_2 and CH_4 differences show biases of 2.5% and 0.7% respectively (OP > in situ). We do not expect zero bias between OP and in situ measurements due to the different natures of the two calibration schemes – the in situ measurements are calibrated against SI-traceable reference standards, whereas the open path measurements rely on retrieval of concentrations from fitting spectra without any possibility for SI-traceable calibration. The accuracy of the OP relative to calibrated in situ measurements is similar in magnitude to that seen in mid IR FTIR studies (Smith et al., 2011; Griffith et al., 2012). After correction for this bias, the apparent 1σ variability in the differences is 2-3 times larger than the OP repeatability, as discussed below. The in situ repeatability is of the order of 0.1% and contributes little to the variability in the differences.

The bottom section of Table 2 presents the sensitivity of concentration retrievals from the spectra to realistic uncertainties in input parameters and choices in the retrieval. Details are given in the caption to Table 2. There is no dominant single source of uncertainty; the main contributors are derived from uncertainties in the Hitran linewidths, the instrument lineshape, stray radiation, and details of the fitted spectral window. A simple quadrature sum of the estimated systematic errors (4.5% for CO_2, 3.3% for CH_4 and 5.9% for O_2) is larger than the observed systematic biases relative to in situ measurements; thus the observed biases are consistent with our a priori estimates of systematic errors.

Data from recent work using broadband DOAS and laser-based long open path techniques are shown for comparison in Table 3. Compared to conventional DOAS with a grating monochromator, array detector and the same long path fibre-telescope optics (Sommer, 2012; Saito et al., 2015; Somekawa et al., 2011), the FTS system achieves greatly improved precision and accuracy. Compared to more recent work with dual frequency comb laser spectroscopy (Rieker et al., 2014; Waxman et al., 2017), the precision is similar. The frequency comb was operated over a longer pathlength with shorter measurement times and achieved better accuracy when compared to co-located in situ measurements, but at this stage of development is less portable for remote field measurements and applicable only to a narrower range of species. The FTS setup has advantages in terms of mobility and costs.

4.2 Comparison of open path and in situ measurements

CO_2

From the histogram in Figure 10(c), the differences between open path and in situ measurements (OP – in situ) have near-normally distributed variability with 2-3 times the standard deviation of the actual measurement noise (2 vs 5 ppm). There is a bias in the mean difference of around -2 ppm and a slight negative tail in the distribution. We interpret these larger differences to reflect true differences between the point and open path measurements. However time series of Figure 9 for CO_2 (upper traces) show that the distribution is not actually random in time, with clear periods of systematic differences that are greater than the measurement precision on synoptic timescales (days). The small negative bias of the distribution can be traced mainly to SE and S wind directions from the nearby main road (Berliner Strasse) and the more distant Heidelberg city centre (Figure 10 (a,b)). This appears to affect the in situ site more than the open path, but generally by less than 5 ppm.

There is no corresponding wind direction for episodes of positive difference, except possibly at times of very low windspeeds (Figure 10a).

CH4

5 For CH$_4$, the distribution of differences (Figure 12(c)) is also near-normal, but with no significant bias and a small positive tail. Although there is no dominant direction associated with positive differences there are several episodes where OP measurements are significantly higher than in situ, for example around 10-11 August and 5 September. The 10-11 August period corresponds to winds from areas of Heidelberg WSW of the measurement path, while 5 September included winds from the NNW that includes the site of a small power station (Figure 2) which would minimally affect the in situ
10 measurements.

The OP-in situ differences and geographical scales of these measurements approach the accuracy and resolution of developing regional scale models such as the Weather Research and Forecasting model (WRF) in high resolution mode (Viatte et al., 2017). A detailed high resolution modelling analysis of the measurements presented here is however beyond the scope of this paper.

15 **4.3 Future improvements**

This study was made with available instrumentation as a pilot study of the open path FTS technique in the NIR and did not optimise some aspects of the measurements. Several options are available to improve the accuracy and precision of the OP-FTS-NIR measurements:

-      Interferences from stray radiation: especially at low solar elevations, background (stray) radiation is modulated and
20 detected by the interferometer and leads to broad enhancements and spikes in measured concentrations. This can be almost entirely removed by reversing the source and detector in the optical system shown in Figure 1, first modulating the source in the interferometer before transmission over the open path. With this option stray environmental radiation such as direct or scattered sunlight is viewed directly by the detector and not modulated by the interferometer; it does not contribute to the Fourier-transformed infrared spectrum. This option was not possible with the available optics and spectrometer for this pilot
25 study, but will be incorporated in the next build. With the present system, increasing the frequency of the background stray light measurements (1 per hour in this work) would allow better correction for stray light interferences due to short term variations in stray radiation, but at the cost of lower precision, measurement time and duty cycle.

-      Increased optical throughput: using a brighter source and/or larger telescope and retroreflector area will translate directly into lower measurement noise and improved precision. This is particularly true of retroreflectors, which had a total
30 area of around 510 cm^{-2} compared to the telescope primary mirror area of 700 cm^2. A close packed retroreflector array large enough to capture the (slightly divergent) open path beam could thus improve precision by a factor of about two for the same primary telescope aperture.

- Extension to include CO: for urban studies the measurement of CO is advantageous, both for its intrinsic interest and as a tracer for combustion sources of other trace gases. In this work we used available UV quartz retroreflectors optimised for UV/vis DOAS measurements. The transmission of UV quartz cuts off below 4500 cm^{-1}, precluding CO measurement in the overtone band around 4300 cm^{-1}. The use of corner cube retroreflectors with transmission to 4000 cm^{-1}

5 (for example hollow mirror, glass or IR quartz) will allow measurements to extend to CO. A simulation with the measurement noise realised in this work suggest a CO measurement precision of a few ppb, which should be sufficient for urban areas.

4.4 Final comments

We have introduced a long open path Fourier Transform spectrometer operating in the near infrared over a 3.1 km return

10 path in open air. The system is able to make measurements of several species simultaneously by virtue of the broadband nature of the spectroscopy. We have demonstrated measurements of CO_2, CH_4, O_2, H_2O and HDO; with a minor variation optics CO is also possible, which would be of advantage in urban environments. The spectrometer is reasonably portable, able to be tripod mounted, and requires power (~ 150 W) and shelter at only one end of the path, with a passive retroreflector array at the far end of the path.

15 We observe differences between the open path and point measurements that are significant relative to the measurement precisions. In the context of fine scale atmospheric models, which now provide kilometre scale resolution, open path measurements have the potential to bridge the gap between high accuracy point measurements and spatially-averaging atmospheric models. With improvements in precision and accuracy to be expected in both broadband (FTS) and laser based techniques, open path spectroscopy provides a valuable new tool for urban and regional scale studies.

5 Acknowledgements

This work was carried out as a sabbatical leave project by DG at the Institute for Environmental Physics, University of Heidelberg. DG thanks Ingeborg Levin, Ulrich Platt and members of the DOAS and carbon cycle groups for their contributions and collaboration in providing the laboratory and long path optical systems for the study. Geoff Toon, JPL,

25 provided updated 2015 versions of GFIT line parameters .

6 References

Aemisegger, F., et al.: Measuring variations of δ^{18}O and δ^{2}H in atmospheric water
    vapour using two commercial laser-based spectrometers: an instrument characterisation study, Atmos. Meas. Tech.,
30   5, 1491-1511, 10.5194/amt-5-1491-2012, 2012.

Frey, M., et al.: Calibration and instrumental line shape characterization of a set of portable FTIR spectrometers for detecting greenhouse gas emissions, Atmospheric Measurement Techniques, 8, 3047–3057, 10.5194/amt-8-3047-2015, 2015.

GLOBAL-VIEW-CO$_2$: Cooperative atmospheric data integration project - carbon dioxide, CD-ROM, also available from ftp.cmdl.noaa.gov, Boulder, Colorado, 2009.

5 Griffith, D. W. T.: Synthetic calibration and quantitative analysis of gas phase infrared spectra, Appl. Spectrosc., 50, 59-70, 1996.

Griffith, D. W. T., et al.: FTIR spectrometry in atmospheric and trace gas analysis, in: Encyclopedia of Analytical Chemistry, edited by: Meyers, R. A., Wiley, 1979-2007, 2006.

Griffith, D. W. T., et al.: A Fourier transform infrared trace gas analyser for atmospheric applications, Atmospheric
10 Measurement Techniques, 5, 2481-2498, 10.5194/amtd-5-3717-2012, 2012.

Hammer, S., et al.: Assessment of a multi-species in situ FTIR for precise atmospheric greenhouse gas observations, Atmospheric Measurement Techniques Discussions, 6, 1153-1170, 2013.

Hase, F., et al.: Analysis of the intrumental lineshape of high resolution FTIR spectrometers with gas cell measurements and new retrieval software, Appl. Opt., 38, 3417-3422, 1999.

15 Lee, J. K., et al.: A mobile sensor network to map carbon dioxide emissions in urban environments, Atmos. Meas. Tech. Discuss., 2016, 1-33, 10.5194/amt-2016-200, 2016.

Merten, A., et al.: Design of differential optical absorption spectroscopy long-path telescopes based on fiber optics, Appl. Opt., 50, 738-754, 2011.

Platt, U., et al.: Differential Optical Absorption Spectroscopy: Principles and Applications, Springer, 2008.

20 Press, W. H., et al.: Numerical Recipes, Cambridge University press, 1992.

Rieker, G. B., et al.: Frequency-comb-based remote sensing of greenhouse gases over kilometer air paths, Optica, 1, 290-298, 10.1364/optica.1.000290, 2014.

Rothman, L. S., et al.: The HITRAN 2008 molecular spectroscopic database, Journal of Quantitative Spectroscopy & Radiative Transfer, 110, 533-572, 2009.

25 Russwurm, G. M., et al.: Open Path Fourier Transform Spectroscopy, in: Handbook of Vibrational Spectroscopy, edited by: Chalmers, J. M., and Griffiths, P. R., John Wiley & Sons Ltf, 2002.

Saito, H., et al.: Near infrared open path measurement of CO$_2$ concentration in the urban atmosphere, Optics Letters, 40, 2568-2571, 2015.

Smith, T. E. L., et al.: Absolute accuracy evaluation and sensitivity analysis of OP-FTIR NLS retrievals of CO$_2$, CH$_4$ and CO
30 over concentrations ranging from those of ambient atmospheres to highly polluted plumes., Atmospheric Measurement Techniques, 4, 97-116, 2011.

Somekawa, T., et al.: Differential optical absorption spectroscopy measurement of CO$_2$ using a nanosecond white light continuum, Optics Letters, 36, 4782-4784, 2011.

Sommer, P.: Optimierung eines Langpfad-Nah-IR DOAS-Aufbaus zur Messung von Wasser, Kohlenstoff Dioxid und
35 Methan in der unteren Troposphaere, B. Sc., Institute for Environmental Physics, University of Heidelberg, 2012.

Toth, R. A., et al.: Spectroscopic database of CO2 line parameters: 4300–7000cm−1, Journal of Quantitative Spectroscopy and Radiative Transfer, 109, 906-921, http://dx.doi.org/10.1016/j.jqsrt.2007.12.004, 2008.

Tuazon, E. C., et al.: A kilometre pathlength Fourier Transform Infrared system for the study of trace pollutants in ambient and synthetic atmospheres, Atmos. Environ., 12, 865-875, 1978.

40 Turner, A. J., et al.: Network design for quantifying urban CO2 emissions: Assessing trade-offs between precision and network density, Atmos. Chem. Phys. Discuss., 2016, 1-20, 10.5194/acp-2016-355, 2016.

Vardag, S. N., et al.: First continuous measurements of δ18O-CO2 in air with a Fourier transform infrared spectrometer, Atmospheric Measurement Techniques, 8, 579-592, 10.5194/amt-8-579-2015, 2015.

Viatte, C., et al.: Methane emissions from dairies in the Los Angeles Basin, Atmos. Chem. Phys., 17, 7509-7528,
45 10.5194/acp-17-7509-2017, 2017.

Waxman, E. M., et al.: Intercomparison of Open-Path Trace Gas Measurements with Two Dual Frequency Comb Spectrometers, Atmos. Meas. Tech. Discuss., 2017, 1-26, 10.5194/amt-2017-62, 2017.

Wunch, D., et al.: Calibration of the Total Carbon Column Observing Network using Aircraft Profile Data, Atmospheric Measurement Techniques, 3, 1351-1362, 2010.

Wunch, D., et al.: The Total Carbon Column Observing Network (TCCON), Philosophical Transactions of the Royal Society A 369, 2087-2112, 2011.

Wunch, D., et al.: The Total Carbon Column Observing Network's GGG2014 Data Version Oak Ridge, Tennessee, U.S.A., 2015.

Tables

Table 1. Details of spectral windows used for fitting. * In O_2 there is also a weak contribution from collision-induced continuum absorption which is fitted with the overall continuum.

Species fitted	Interfering species co-fitted	Spectral region cm^{-1}	Spectral region μm
O_2	H_2O *	7790 – 7960	1.26 – 1.28
CO_2	H_2O	4800 - 5050	1.99 – 2.04
CH_4	H_2O	5885 - 6150	1.63 – 1.70
H_2O, HDO	CO_2	4910 – 5080	1.97 – 2.04

Table 2. Precision, accuracy and sensitivity to retrieval inputs in the OP-FTIR measurements. For discussion of precision and accuracy, see text. For the sensitivity to systematic errors, each input parameter or choice was varied by an estimate of its uncertainty in the MALT spectrum analysis and its effect on retrieved mole fractions calculated.

			δCO_2		δCH_4		δO_2	
			ppm	%	ppb	%	mol. frac.	%
OP measurement repeatability								
Variability (1σ, 5 min)			1.5	0.4%	40	2.2%	0.0052	2.5%
Differences to in situ measurements								
Variability (1σ, 5 min)			5	1.2%	93	5.2%		
Bias			10	2.5%	13	0.7%	0.0175	3.6%
Sensitivity of retrieval to systematic errors								
Quantity	**δ**	**δ%**						
[1]Temperature	+3°C	+1%	+6.04	1.4%	+24.7	1.3%	+0.0032	1.5%
[1]Pressure	+1.0 mb	+0.1%	-0.69	0.2%	-2.0	0.1%	-0.0002	0.1%
[2]Pathlength	+ 3 m	+0.1%	-0.4	0.1%	-1.8	0.1%	-0.0002	0.1%
[3]Linestrengths		+2%	-8.0	2%	-36	2%	-0.002 ()	2%
[3]Linewidths		+2%	-4.88	1.2%	+5.4	0.3%	-0.0004	0.2%
[4]Zero offset	+0.01	+1%	+10.5	2.5%	+21.0	1.1%	0.0029	1.4%
[5]ILS width		+5%	+5.0	1.2%			0.0079	3.8%
[6]Window selection				2%		2%		2%
[6]Continuum polynomial				1%		0.1%		3%
[7]Fibre Residual				<<1%		<<1%		<<1%
Quadrature sum				**4.5%**		**3.3%**		**5.9%**

[1] Temperature and pressure errors affect retrieved mole fractions in two ways – proportionally through the dilution of air to calculate mole fraction from concentrations, and through the temperature and pressure sensitivities of linestrengths and lineshapes. From the net sensitivities, it can be seen that the errors are dominated by the dilution effects.

[2] Pathlength error propagates proportionally into the path average mole fraction, since the spectrum analysis retrieves the concentration- pathlength product.

[3] We estimate for a 2% error on Hitran linestrengths and linewidths – these errors are not well characterised (Toth et al., 2008).

[4] Adding a zero offset of 1% to the spectrum simulates the effect of 1% stray sunlight added to the spectrum, and can be taken as an estimate of the maximum effect due to stray light.

[5] The Instrument Line Shape (ILS) is fitted for every spectrum by allowing the FTIR field of view (FOV), phase error and frequency shift to vary in the least squares minimisation. The quoted error is calculated by forcing the width to increase by 5% above the best-fit value to estimate the effect of a non-ideal ILS.

[6] The selection of spectrum window to be fitted, and the number of terms in the polynomial used to fit the continuum, is somewhat subjective – the selections are based on visual assessment of the spectral residual and the minimum mean residual achieved. The sensitivity taken from the variation in retrieved concentrations across a range of "acceptable" window and baseline choices. Note the continuum choice for O_2 is more sensitive because the polynomial is effectively used to fit the unstructured pressure-induced continuum in the O_2 spectrum. Although we measured short path spectra every hour, in principle to characterise the continuum spectrum, using these spectra to define the continuum rather than fitting it did not improve fits, but added noise and an extra source of variability. All results were thus obtained with the continuum fitted with a 5-term polynomial.

[7] The fibre optic coupling between telescope, source and detector introduces repeatable fringing and interferences in the measured spectra at about 1% of the measured signal intensity. These structures can be seen in the residual plots of Figure 4 and are quite reproducible over periods of days to weeks. They are larger than the underlying detector noise but much less than the trace gas absorptions, at least for CO_2 and O_2. Removing or co-fitting an average fibre residual spectrum during the fit makes only a small (<<1%) difference to the retrieved mole fractions because the fibre residual spectrum is itself derived from the least squares fits to real spectra and is approximately orthogonal to the target gas spectrum.

Table 3. Comparison of precision and accuracy of long path techniques in the NIR region. [1] (Sommer, 2012; Saito et al., 2015; Somekawa et al., 2011); [2] (Rieker et al., 2014; Waxman et al., 2017)

	CO_2 / ppm			CH_4 / ppb		
	Meas. Noise (1σ, 5 min)	OP – in situ		Meas. Noise (1σ, 5 min)	OP – in situ	
		Variability (1σ)	Bias		Variability (1σ)	Bias
FTS (this work)	1-2	5	10	40	93	13
DOAS[1]	2-4	-	-	>200	-	>200
Freq. Comb[2]	<1	-	3- 6	<5	-	4-20
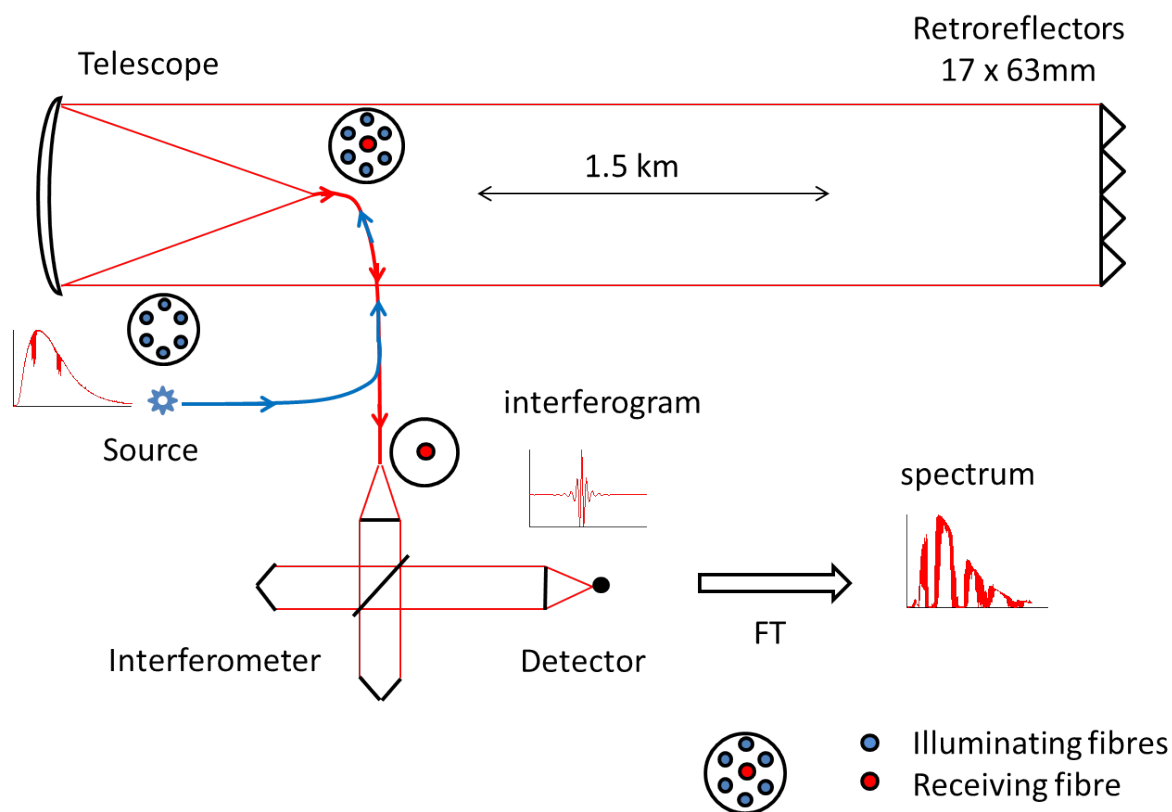
Figures

Figure 1. Schematic drawing of the long open path FT spectrometer and optical system. Radiation from the source is fed close to the focus of the telescope through the outer bundle of six fibres (blue) and transmitted across the open path. The return beam is collected by the central fibre (red) and focussed onto the input aperture of the interferometer. The modulated beam from the interferometer is detected by the InGaAs detector and the resultant interferogram is Fourier transformed to provide the long open path spectrum.
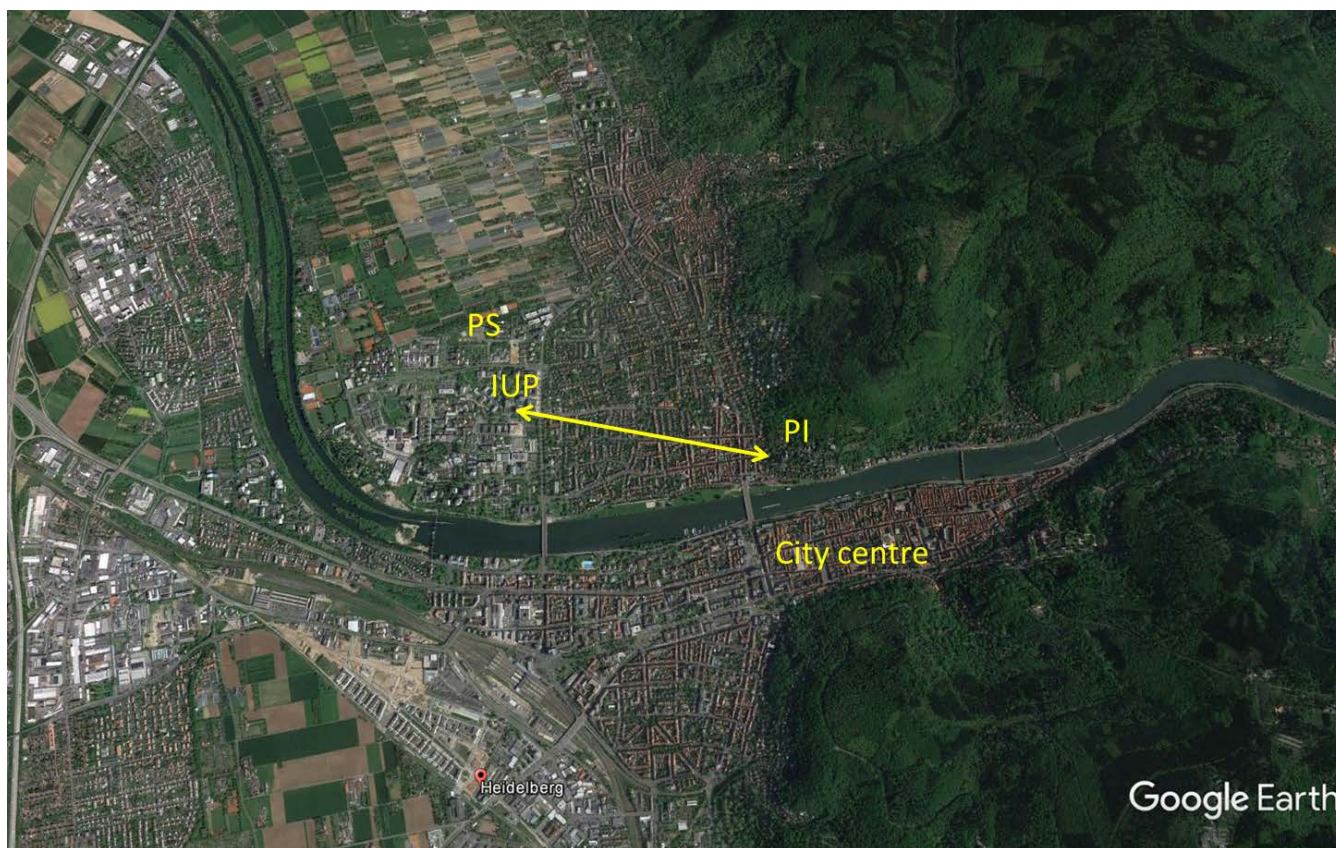
Figure 2. Aerial view of Heidelberg and the 1.5 km measurement path. IUP = Institute of Physics (FTS and telescope), PI = Physics Institute (retroreflector), PS = power station.
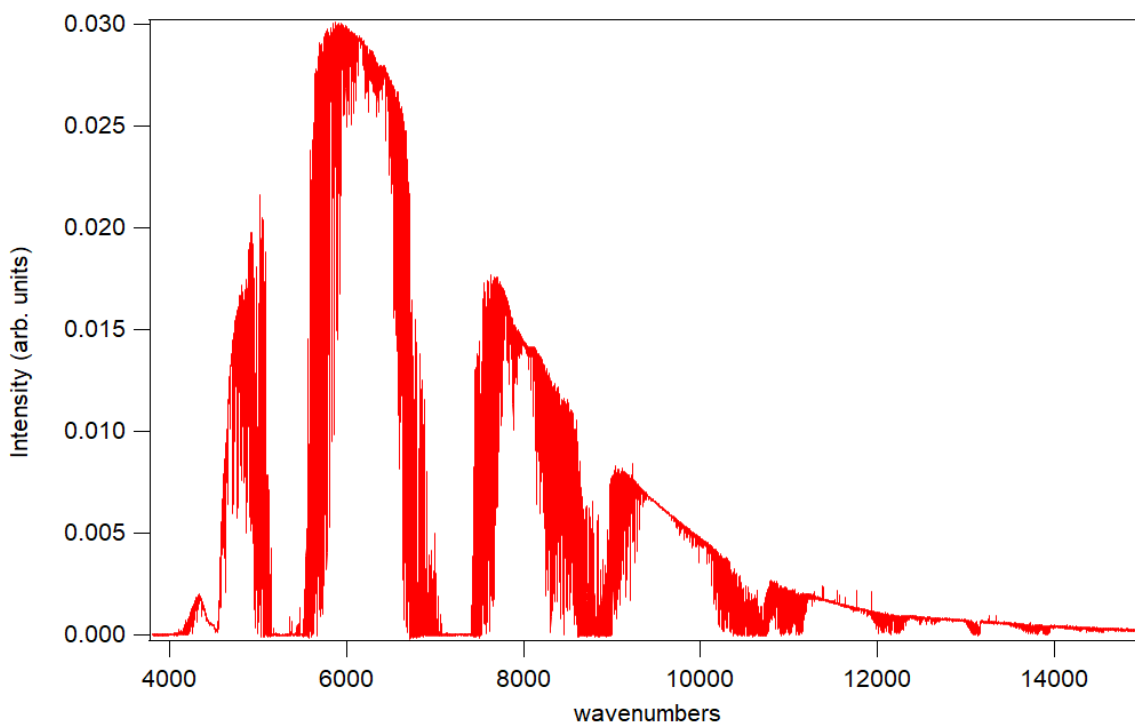
5   **Figure 3. Typical NIR long path spectrum, recorded 01 Oct 2014.**
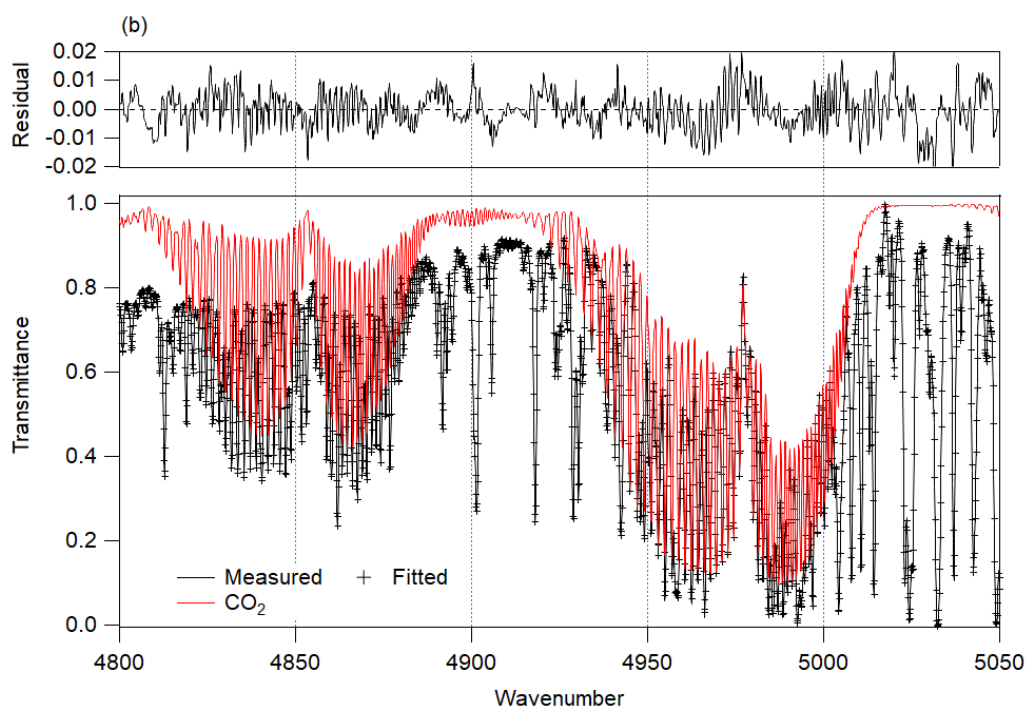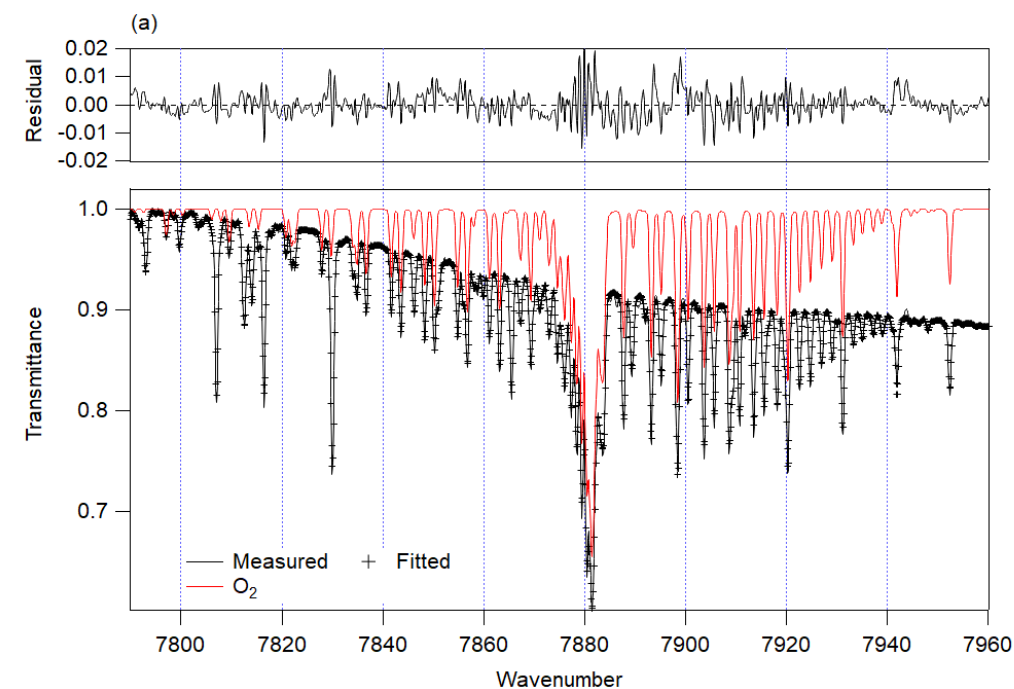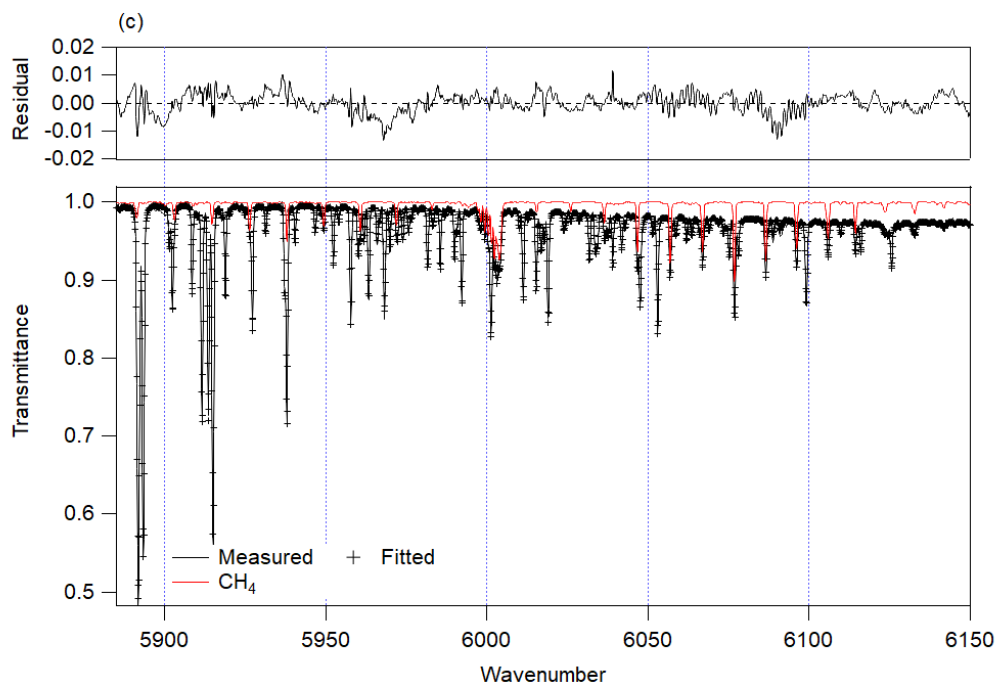
Figure 4. Typical fits for (a) O$_2$ band centred near 7880cm^{-1} (b) CO$_2$ bands centred near 4850 and 4980 cm^{-1} and (c) CH$_4$ band centred near 6000 cm^{-1}.
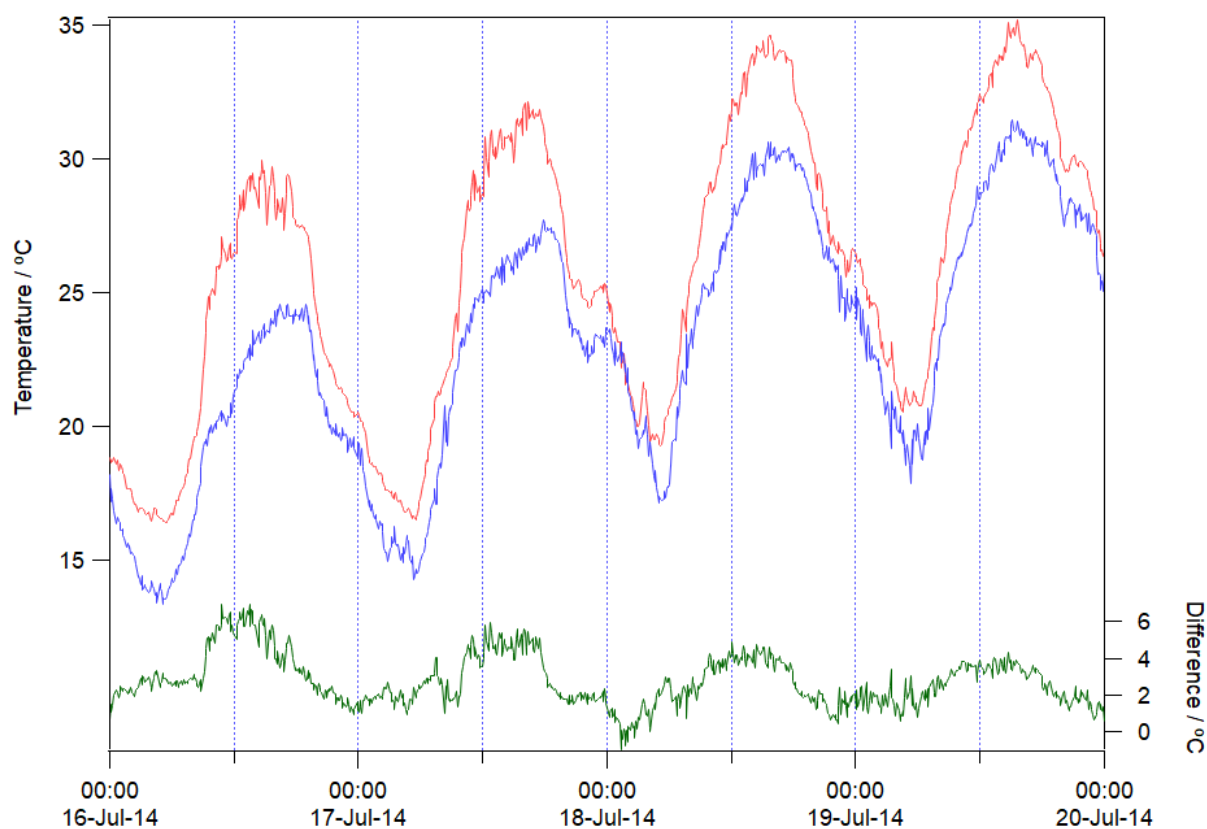
Figure 5. Comparison of IUP meteorological station temperature (red) and spectrum-derived path averaged temperature (blue)
5   **for an illustrative period of 4 sunny days. The differences are plotted in green and range from 0 – 6 °C.**
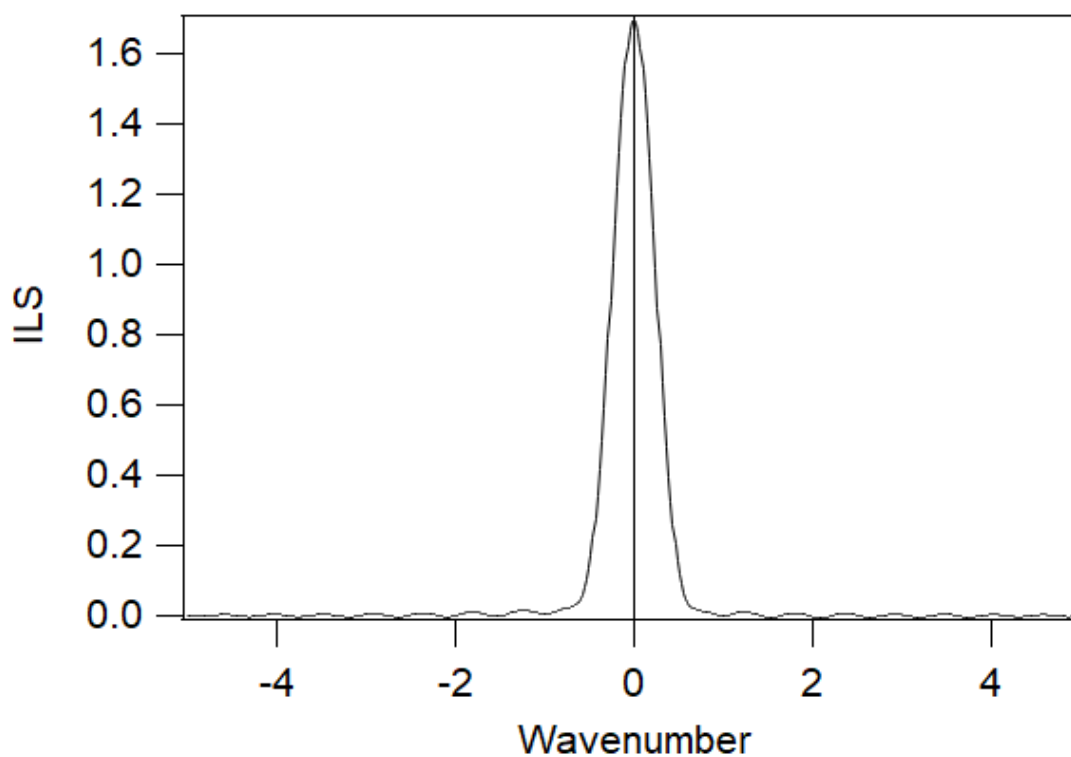
5   **Figure 6. Retrieved instrument lineshape function for the IRcube FTS at 0.5 cm^{-1} resolution.**
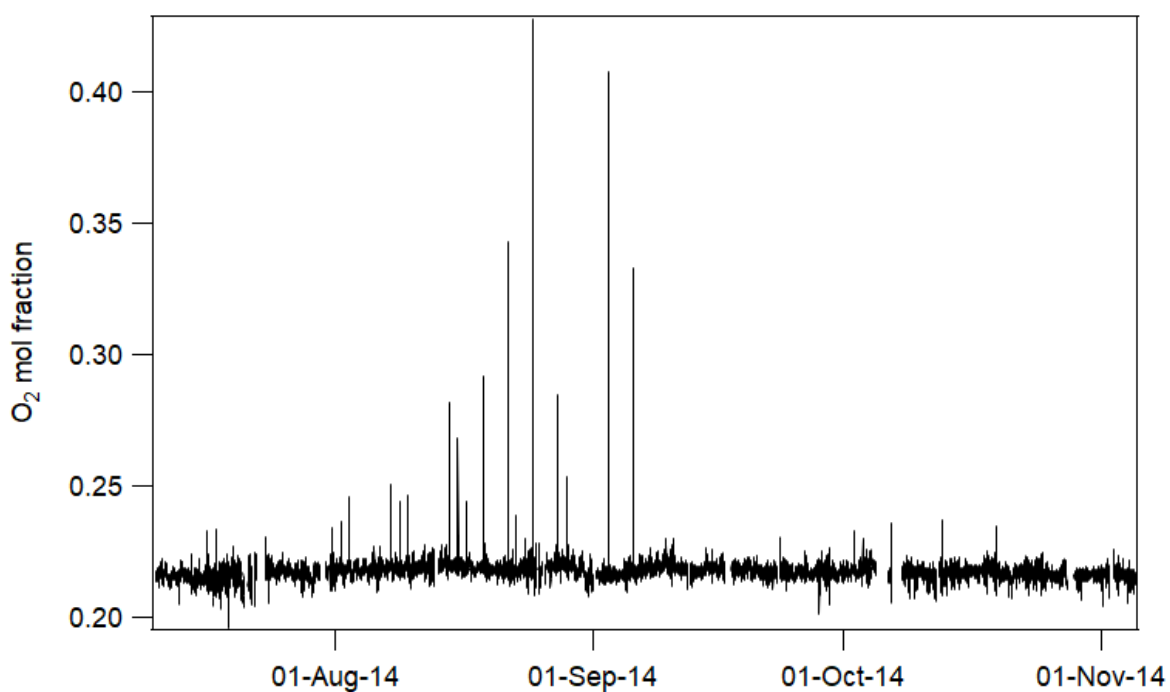
Figure 7. Measured O$_2$ mole fractions for the measurement period. The narrow spikes are artefacts due to stray solar radiation near 18:00 on sunny days, as discussed in the text.
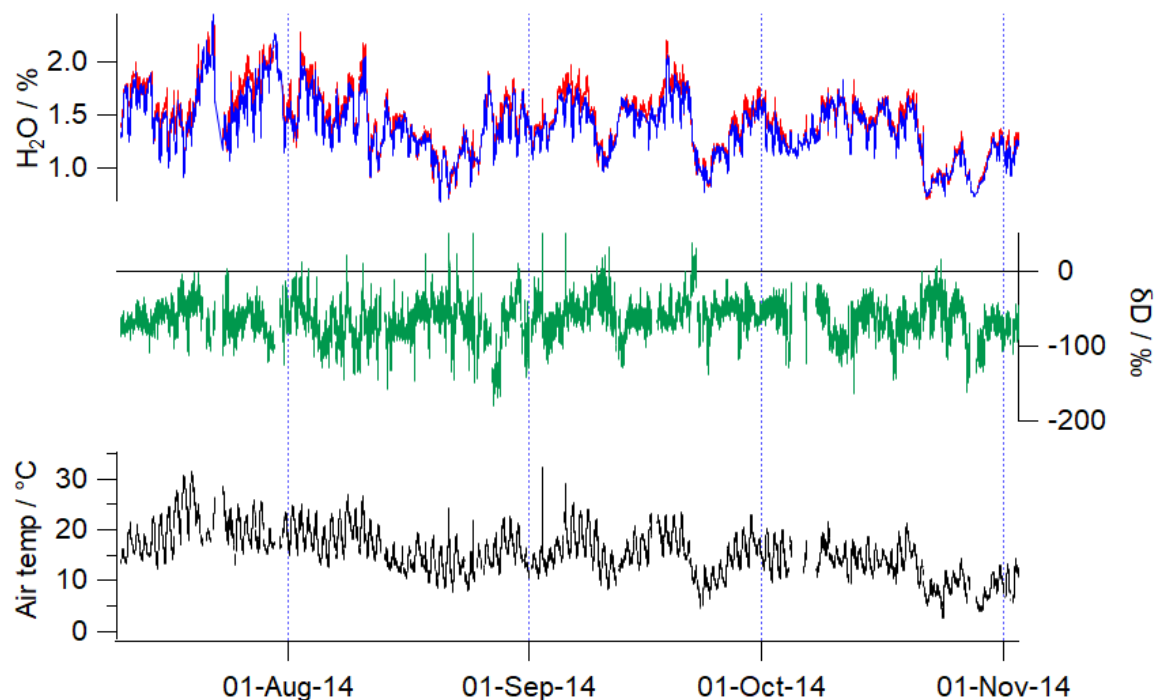
5   **Figure 8. Water vapour, δD and air temperature for the whole measurement period. In the upper panel the FTIR retrieved water vapour is in red and the IUP meteorological station absolute humidity in blue (as mole fractions in %).**
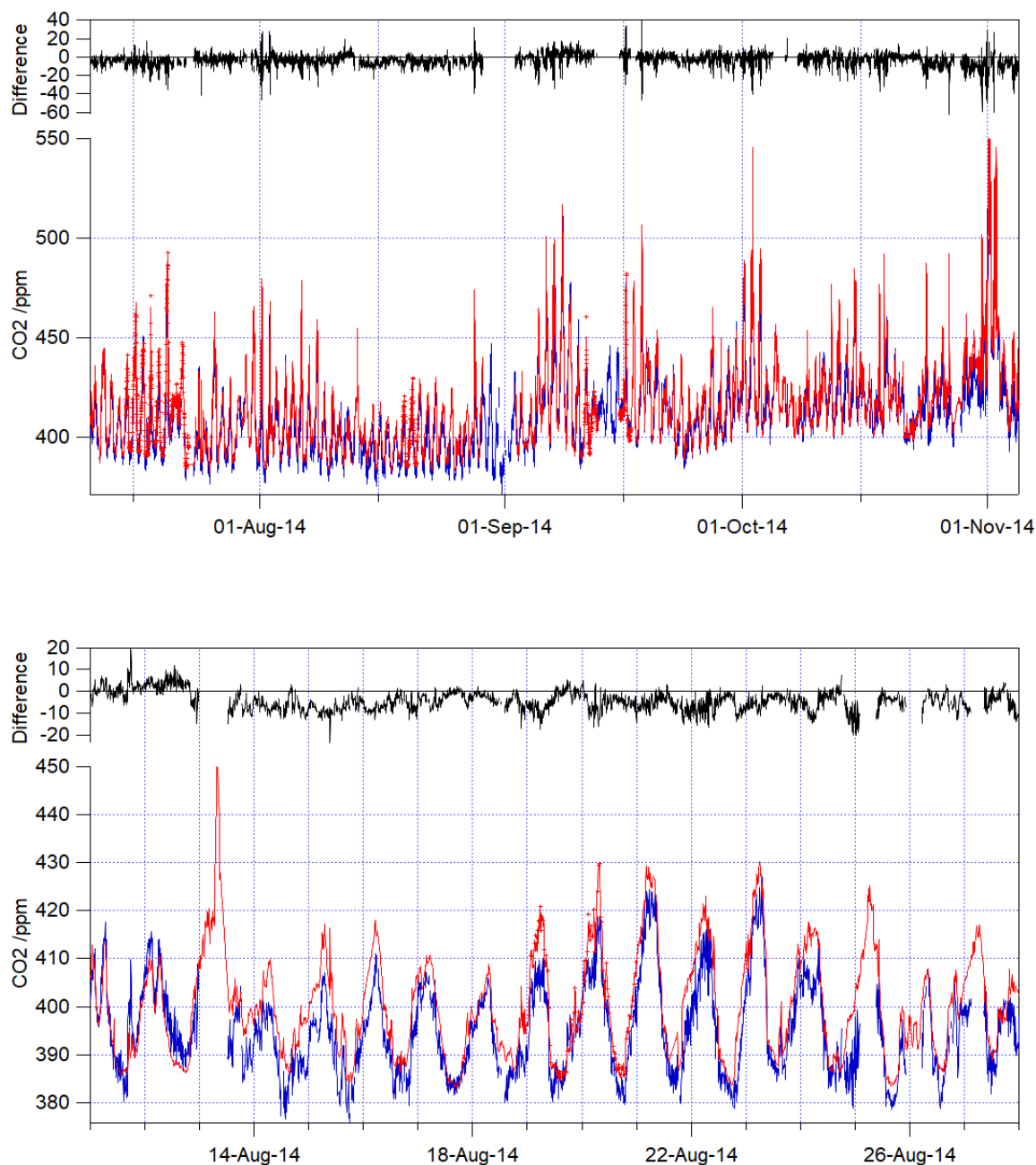
5   **Figure 9. Open path (blue), in situ (red) and difference (OP – in situ, black) measurements of CO_2. All raw OP data have been reduced by a factor of 1.025 (~ 10 ppm) to remove measurement bias relative to the in situ data. In the corrected data, there is zero bias for wind speeds > 6 m s-1 over the entire measurement period (see text for detail). (a) shows the whole measurement period. (b) illustrates a selected period with a consistent, real OP-in situ difference relative to the well mixed average.**
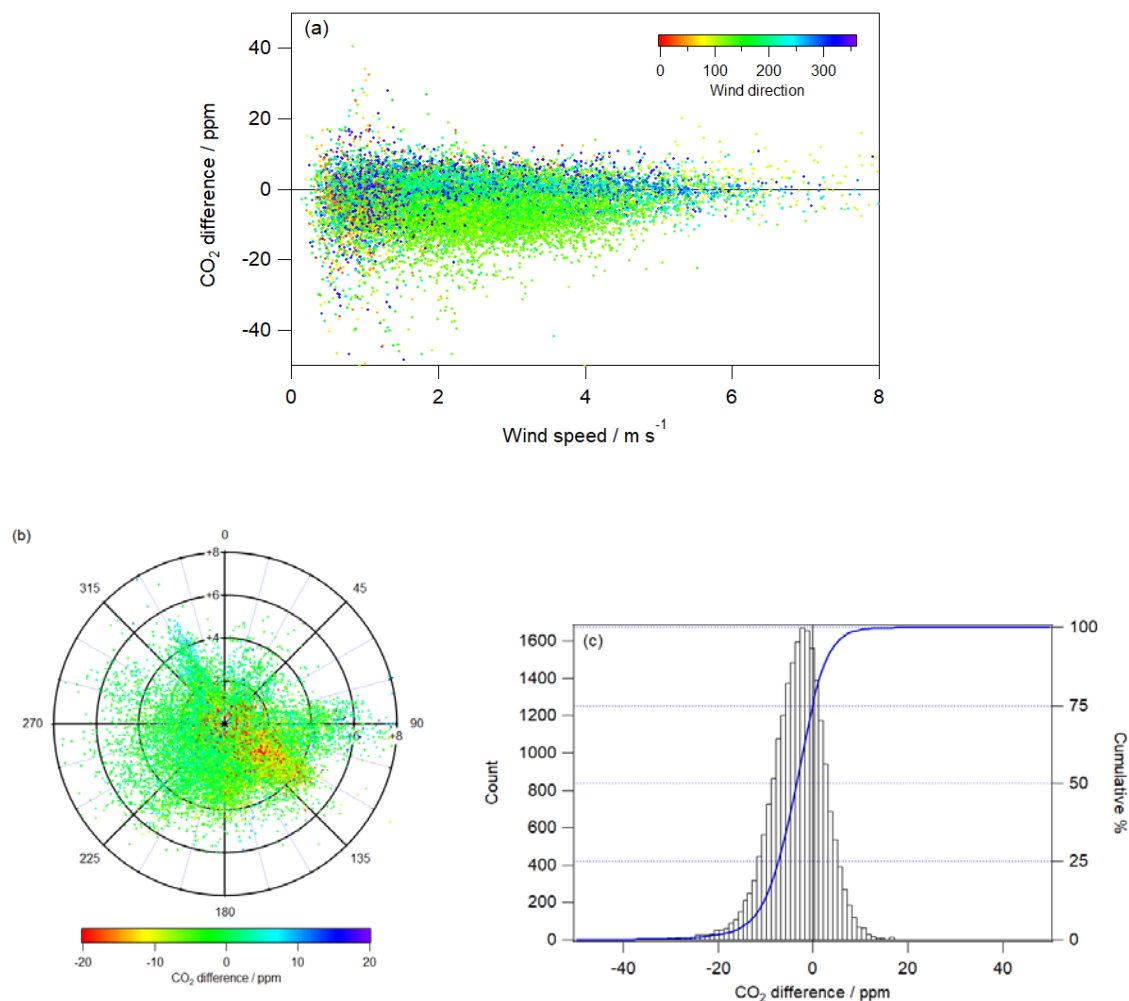
Figure 10. CO_2 mole fraction differences between open path and in situ measurements (OP – in situ) (a) vs wind speed, coloured by wind direction (b) as a wind speed rose, coloured by CO_2 difference, and (c) as a histogram of the differences.
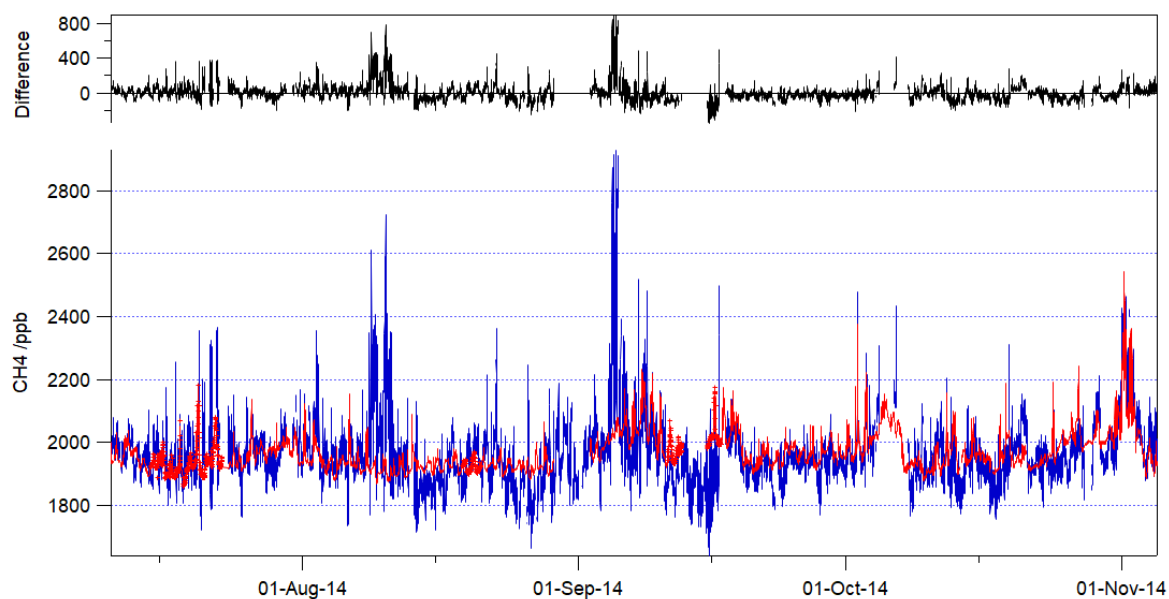
Figure 11. Open path (blue), in situ (red) and difference (OP – in situ, black) measurements of CH₄ for the whole measurement period. The uncalibrated OP data have been reduced by a factor of 1.007 (~13.8 ppb) to fit the in situ data for wind speeds > 2 m s-1 (see text).
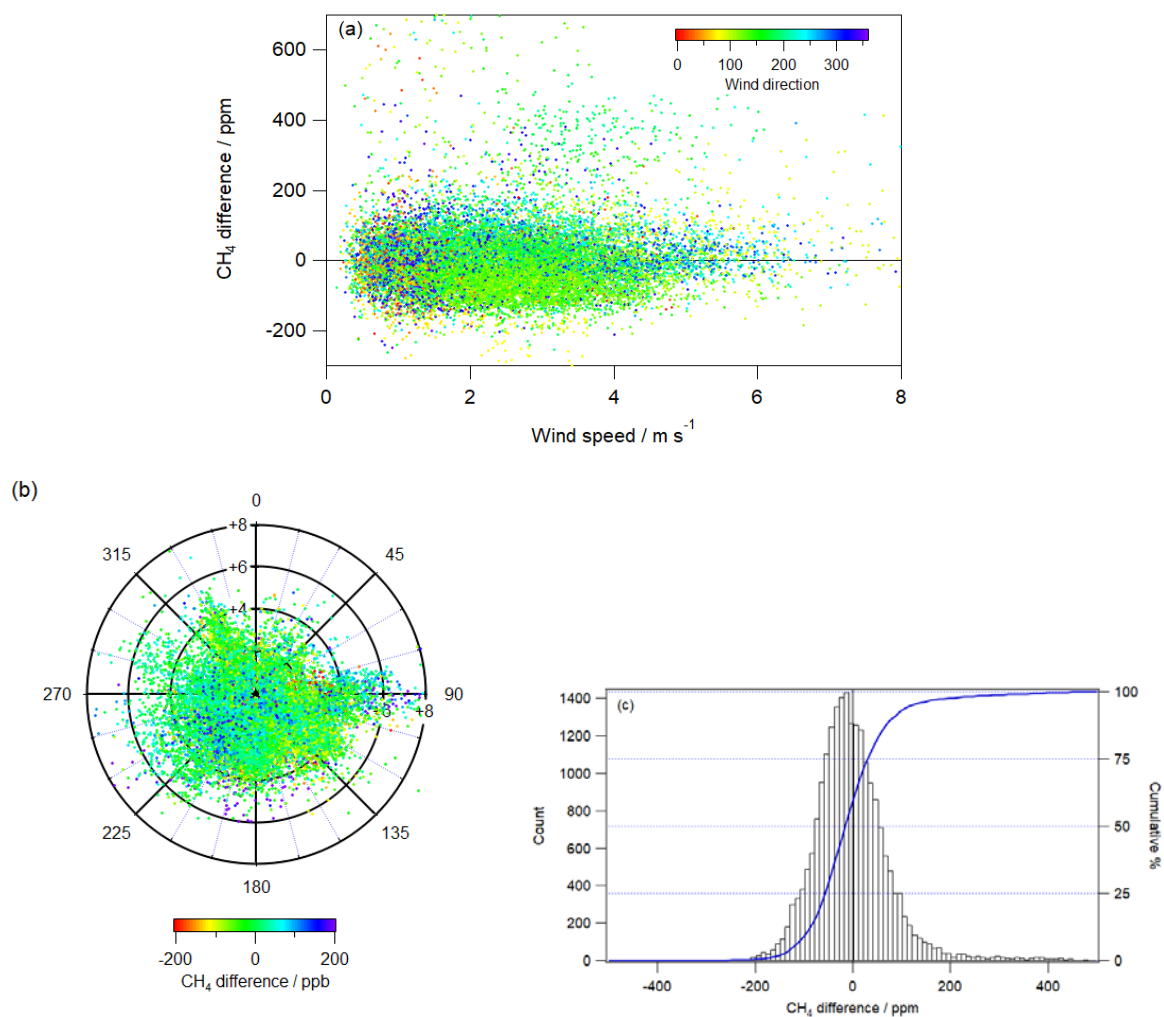
Figure 12. CH$_4$ mole fraction differences between open path and in situ measurements (OP – in situ) (a) vs wind speed, coloured by wind direction (b) as a wind speed rose, coloured by CH$_4$ difference, and (c) as a histogram of the differences.